Available online at www.sciencedirect.com
SCIENCE DIRECT
Trans. Nonferrous Met. Soc. China 18(2008) 493−498
Transactions of Nonferrous Metals Society of China
www.csu.edu.cn/ysxb/

Oxidation of pre-oxidized GH128 alloy implanted with Ce^+ at 1 000 ℃

LI Mei-shuan(李美栓)[1], QIAN Yu-hai(钱余海)[1, 2], ZHOU Yan-chun(周延春)[1]

1. Shenyang National Laboratory for Materials Science, Institute of Metal Research, Chinese Academy of Sciences, Shenyang 110016, China;
2. Technology Center, Baoshan Iron & Steel Company Ltd., Shanghai 201900, China

Received 25 July 2007; accepted 13 September 2007

Abstract: The influence of Ce implantation into preformed scales with a dose of 1×10^{17} ions/cm^2 on the subsequent oxidation behavior of GH128 alloy at 1 000 ℃ in air was investigated. The pre-oxidation was carried out at 1 000 ℃ in air for 1 h and 5 h respectively. Cr_2O_3, NiO and $NiCr_2O_4$ formed on the surface of all specimens. Ce implantation decreased the subsequent oxidation rate of both the alloy and the 1 h pre-oxidized alloy, however, had no effect on that of the 5 h pre-oxidized alloy. The beneficial effect was most obvious in the directly implanted alloy. During the cyclic oxidation for 600 h, Ce implantation for all specimens with or without preferential oxidation played a similar beneficial effect on the oxide spallation resistance. The results indicate that Ce incorporated into the oxide scales affects the diffusion of the reaction species to some extent, the wavy interface and small grain structure make a significant contribution to improving the spallation resistance of the oxide scales.

Key words: oxidation; Ce; ion implantation; GH128 alloy

1 Introduction

It was observed that the additions of small quantities of reactive elements such as rare earth elements(REs), Ti, Zr and Hf into high temperature alloys can decrease the oxidation rate and improve the oxide adherence[1−2]. A number of mechanisms were proposed to explain the so called reactive element effect (REE), of which the modification to oxide growth processes[3−5] and "sulfur" effect[6−7] are generally considered. A great number of investigations supported the two models. However, the relationships of the presence of REs with oxidation process modification and oxide adhesion improvement, and independence of the above two mechanisms have not been verified directly.

One kind of oxidation tests, in which REs are implanted into preformed oxides, may be worth while to clarify the above problems[8−11]. In this test condition, the scale grain boundaries were doped with implants but without a dopant at the metal/scale interface. Therefore, the existence of REs and interfacial segregation of sulfur may happen at the same time. The results obtained by HOU et al[8] indicated that Y implantation into a pre-formed Cr_2O_3 scale on Ni-25%Cr (mass fraction) reduced the subsequent oxidation rate at 1 000 ℃ to a similar content to that for implantation into the alloy, but no improvement in scale adhesion. PAÚL et al[9] found that Ce implantation of 0.9×10^{16} ions/cm^2 both into AISI type 304 stainless steel and into the preformed scale decreased the oxidation rate at 1 173 K similarly. In our previous work[10−11], a dose of 1×10^{17} Ce^+/cm^2 was implanted into the pre-oxidized Ni-20%Cr alloy. The subsequent oxidation rate at 1 050 ℃ was decreased and the oxide adhesion was improved, but the beneficial effects were weaker than that in the direct implantation into the alloy. All above results showed that the presence of REs only in the part layer of oxide scales could play a beneficial role for decreasing the oxidation rate.

In order to further definite the effect of REs implantation into preformed oxides on the subsequent oxidation, another main Cr_2O_3 forming GH128 alloy was investigated in present work. The pre-oxidation and cyclic oxidation were carried out for long time up to 5 h and 600 h, respectively. Ce distribution in the oxide scales was analyzed before and after the subsequent oxidation using SIMS technique.

Foundation item: Project(50571106) supported by the National Natural Science Foundation of China
Corresponding author: LI Mei-shuan; Tel: +86-24-23971145; E-mail: mshli@imr.ac.cn

2 Experimental

The GH128 alloy had the following nominal chemical compositions (mass fraction, %): Cr 22, W 9.0, Mo 9.0, Al 0.8, Ti 0.8, C≤0.05, Fe≤1.0, Zr≤0.06, B≤0.05, Ce≤0.05, Mn≤0.05, Si≤0.08, Ni balance. Single austenite phase and secondary phases of M_6C and TiN existed in the alloy. The dimension of specimens with a hole of *d*2 mm was 12 mm×10 mm×1.5 mm. The surface of the specimens was ground by 600 grit paper, and degreased in acetone ultrasonically followed by ethanol cleaning before oxidation or implantation. The specimens was pre-oxidized at 1 000 ℃ in air for 1 h and 5 h, respectively, and then cooled down to room temperature slowly in the furnace. The preformed oxide scales were integrate and compact. The pre-oxidized specimens and the blank specimens were implanted with a dose of 1×10^{17} Ce^+/cm^2 using the metal vapor vacuum arc (MEVVA) equipment with high-current metal-ion source. During the implantation, a voltage of 50 kV and a beam current of 2.3 mA were used.

The subsequent isothermal and cyclic oxidations were conducted at 1 000 ℃ in air by the thermal microbalance (Setaram, Mtb10-8) and the automatic cyclic oxidation facility with a vertical tube furnace respectively. During the cyclic oxidation, the specimen was quickly put into the furnace at 1 000 ℃ and kept for 1 h, afterwards drawn out to rapidly cool in air for 10 min. An analysis balance (Sartorius BP211D) with a sensitivity of 10^{-5} g was used to measure the mass of the specimen at intervals during the test. The mass change of the specimen with cyclic times (or oxidation time) can be obtained.

After the oxidation, the oxide phases and surface morphologies of specimens were investigated by using X-ray diffractometer (XRD, Philips PW1700), scanning electron microscope equipped with energy dispersive spectroscopy (SEM/EDS, Philips XL30). The depth distribution of Ce was analyzed by secondary ion mass spectroscope (SIMS, Cameco IMS 6F). In the SIMS analysis, the primary ion beam of O^{2+} was used. The acceleration voltage of 15.07 kV, primary ion beam current of 1.99 μA and sputtered area of 250 μm×250 μm were selected.

3 Results and discussion

3.1 Oxidation kinetics

The isothermal oxidation kinetics of the implanted and the un-implanted GH128 alloys at 1 000 ℃ are presented in Fig.1. For the pre-oxidized specimens, the mass gains have been considered in their oxidation kinetics during the pre-oxidation. The mass gains of the specimens are also listed in Table 1. As expected, Ce implantation into the alloy decreases the oxidation rate of GH128 alloy remarkably. Ce implantation into the 1h preformed oxide scale also reduces the subsequent oxidation rate, but this beneficial effect is less notable than that of Ce implantation into the alloy. No positive effect is found when Ce is implanted into 5 h preformed oxide scale. The above results are partly different from that obtained by HOU et al[8], but are consistent with our previous work[10]. And it is further indicated that when the pre-oxidation time is elongated sufficiently or the preformed oxide scale is thick enough, Ce implantation becomes almost ineffective on oxidation rate.

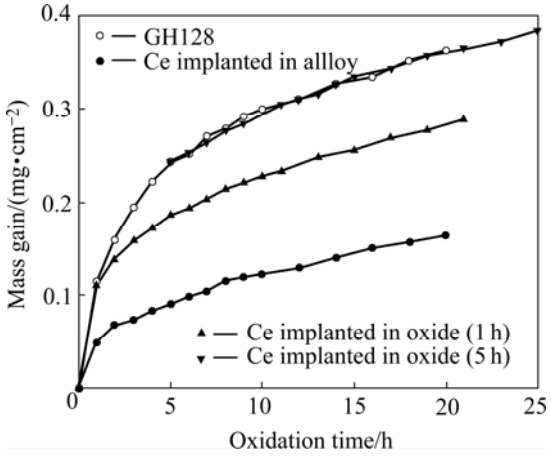

Fig.1 Plots of mass gain vs time during oxidation of blank and pre-treated GH128 alloys at 1 000 ℃ in air

Table 1 Mass gain and oxide thickness of specimens after oxidation

Sample	Mass gain/(mg·cm^{-2})		Oxide thickness/μm*	
	Pre-oxidation	Whole oxidation	Pre-oxidation	Whole oxidation
GH128	−	0.36 (20 h)	−	1.8 (20 h)
Ce implanted in alloy	−	0.16 (20 h)	−	0.4 (20 h)
Ce implanted in oxide (1 h)	0.11 (1 h)	0.28 (20 h) 0.29 (21 h)	0.6 (1 h)	0.9 (21 h)
Ce implanted in oxide (5 h)	0.24 (5 h)	0.36 (20 h) 0.38 (25 h)	1.3 (5 h)	2.2 (25 h)

* Oxide thickness is determined on cross section of specimens by SEM

It should be mentioned that GH128 substrate contains less than 0.05%(mass fraction) Ce. Normally, the effective addition of REs is in the range of 0.1%−0.5% (mass fraction). The content of Ce in GH128 alloy is much lower than that required for performing REE effectively[1−2].

The cyclic oxidation was conducted at 1 000 ℃ in air for 600 h. The kinetic data are illustrated in Fig.2. The mass gain of GH128 decreases continually after 125 h,

which indicates that the oxide scale has serious spallation. However, all of Ce implanted specimens with or without pre-oxidation show a similar cyclic oxidation behavior that presents continuous mass gain in the period of 600 h. Therefore, Ce implantation both into the alloy and into the pre-formed scales can improve the spallation resistance of the oxide scales.

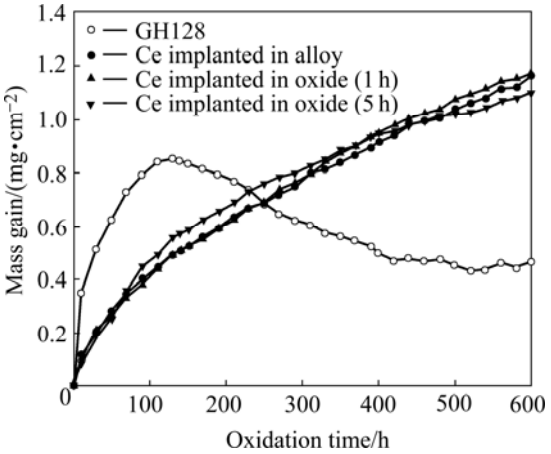

Fig.2 Cyclic oxidation kinetics of blank and pre-treated GH128 alloy at 1 000 ℃ in air

3.2 Oxide phases and scale morphologies

The XRD analysis indicates that after the isothermal subsequent oxidation at 1 000 ℃ in air for 20 h, Cr_2O_3, NiO and $NiCr_2O_4$ are formed on all specimens.

The morphologies of surface and cross sections of the oxide scales formed during the isothermal oxidation are presented in Fig.3 and Fig.4 respectively. All oxide scales do not crack or spall. The oxide scales formed on the two pre-oxidized and then implanted specimens have a similar convoluted surface morphology, and the oxide grains are much smaller than that of GH128 alloy. The oxide/alloy interfaces for three Ce implanted specimens are very wavy. The mean oxide thickness was determined by SEM on the cross section of specimens, and the measured data are also presented in Table 1.

Fig.5 shows the surface morphologies of specimens after the cyclic oxidation for 600 h. The oxide scales on GH128 spall severely; however, on other three Ce implanted specimens the oxide scales crack and spall only in the local small area.

3.3 Alloying element distribution

The depth profiles of alloying elements in the three specimens were analyzed by using SIMS, and the data are shown in Fig.6. In this figure, the position of the oxide/alloy interface was estimated by the profile of Cr or Ni and the measured oxide thickness, and the sputtering rate was roughly 0.86 nm/s.

As shown in Fig.6(a), a peak of Ce content is located near the surface of the preformed scale. Ce depth profile has a long tail. This phenomenon is generally observed because of the limitation of ion sputtering in SIMS. In general, the implanted RE ions distribute according to Gaussian law, and locate within 1−100 nm from the surface of implanted metals[12]. According to Gaussian law, the fitting of the Ce distribution in Fig.6(a)

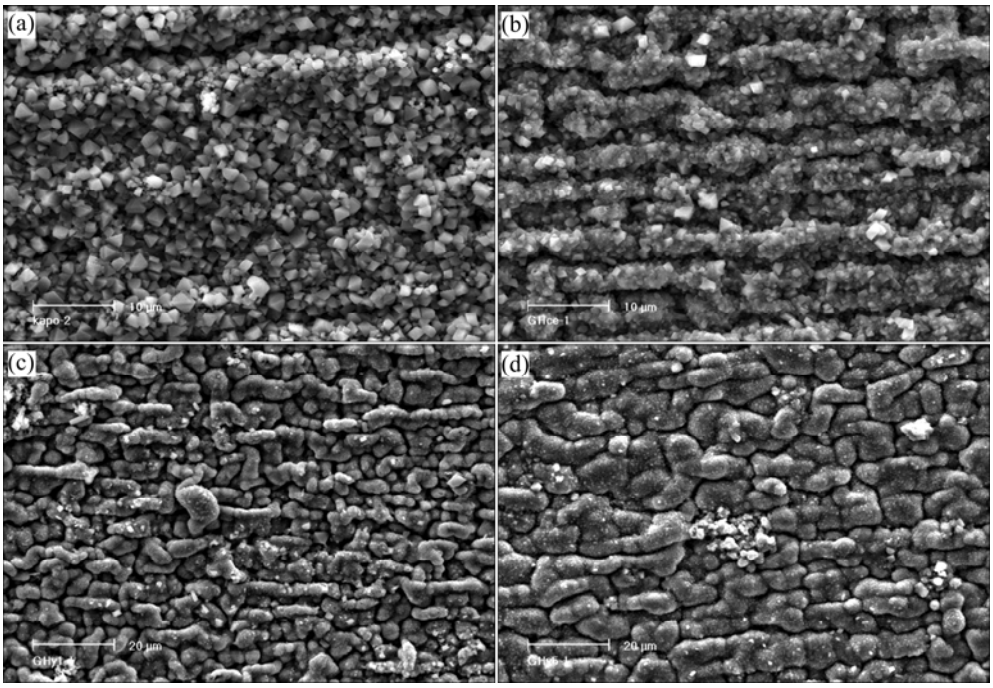

Fig.3 Surface morphologies of specimens after subsequent oxidation at 1 000 ℃ for 20 h: (a) GH128; (b) Implanted with Ce^+; (c), (d) Pre-oxidized for 1 h and 5 h respectively and then implanted with Ce^+

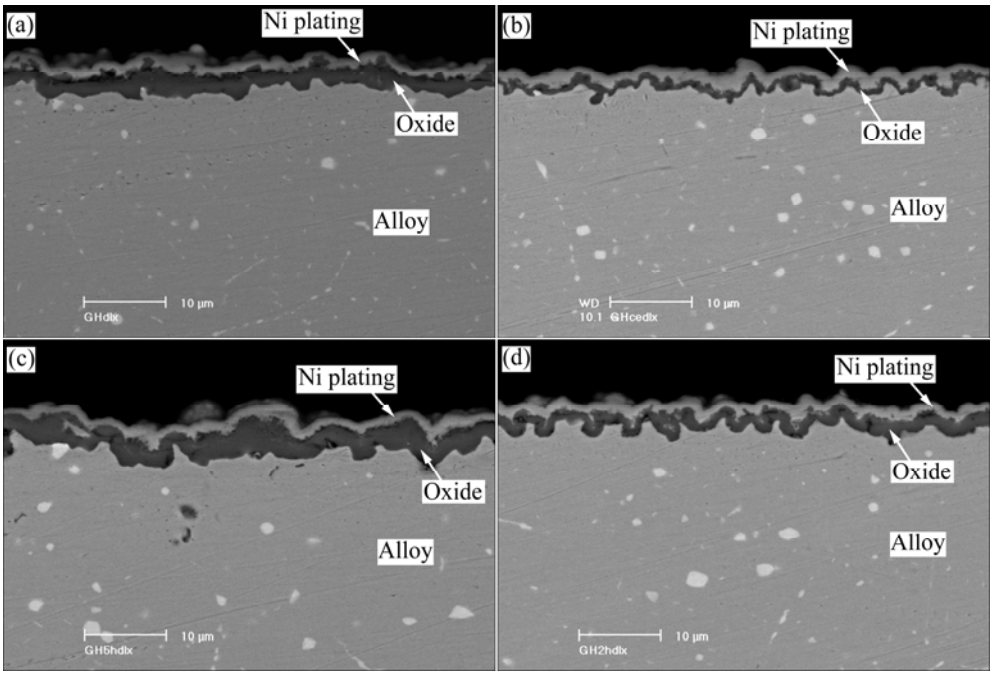

Fig.4 Cross sectional morphologies of specimens after subsequent oxidation at 1 000 ℃ for 20 h: (a) GH128; (b) Implanted with Ce^{+}; (c), (d) Pre-oxidized for 1 h and 5 h respectively and then implanted with Ce^{+}

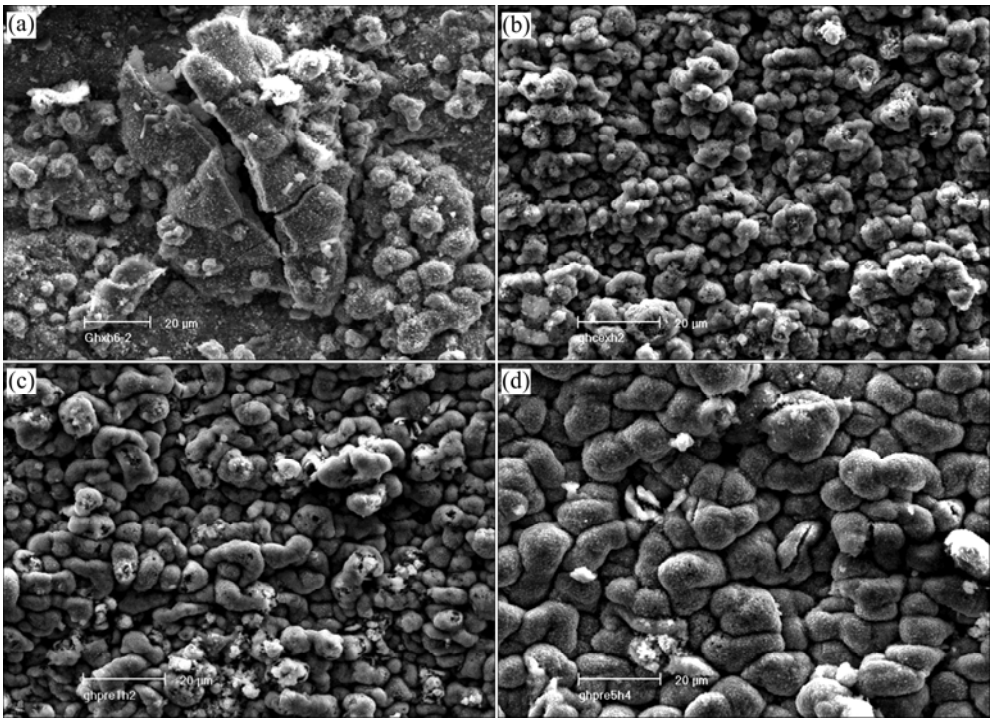

Fig.5 Surface morphologies of samples after cyclic oxidation at 1 000 ℃ for 600 h: (a) GH128; (b) Implanted with Ce^{+}; (c), (d) Pre-oxidized for 1 h and 5 h respectively and then implanted with Ce^{+}

indicates that the depth of implanted Ce does not beyond 0.3 μm. The thickness of the preformed oxide scale is about 0.6 and 1.3 μm for 1 h and 5 h oxidation, respectively. Therefore, the implanted Ce only exists in the outer layer of the preformed oxide, and does not exist at the preformed oxide/alloy interface. In the Ce directly implanted specimen, two peaks of Ce distribution appear. One peak is located in the interior of the scale, the other is situated at the oxide/alloy interface, at which Cr is depleted and Ni and Fe are rich. In the 1 h pre-oxidized and then implanted specimen, Ce distributes evenly in the outer region of the scale, and its content at the oxide/

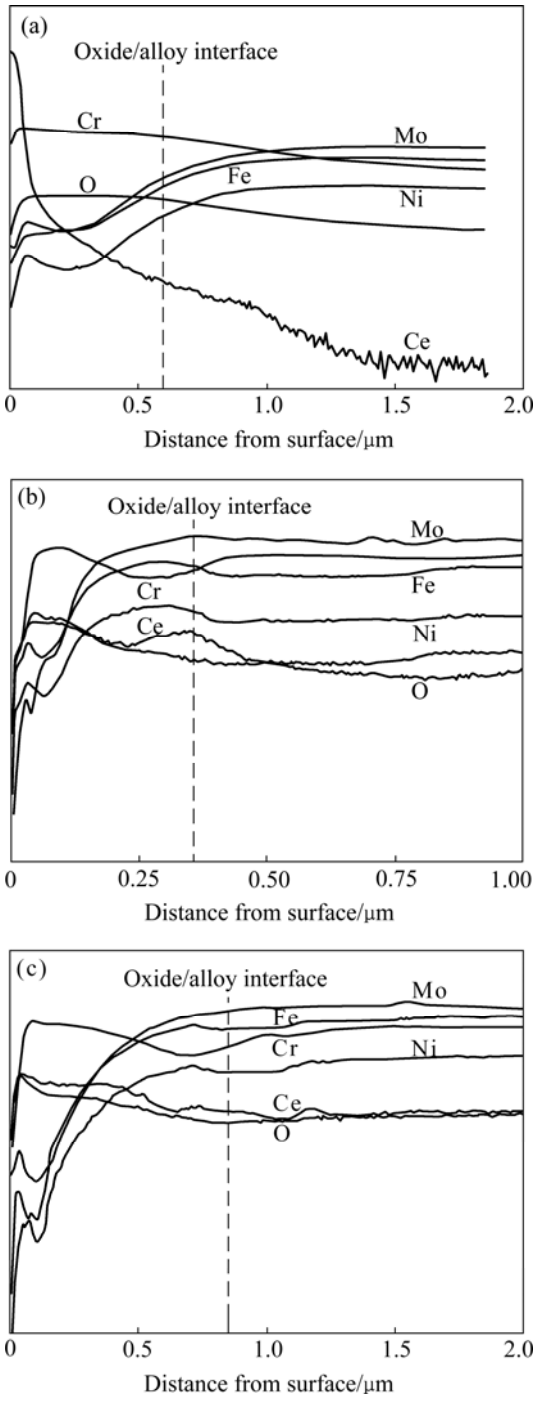

Fig.6 SIMS depth profiles of alloying elements in different treated GH128: (a) 1 h pre-oxidized and then Ce^+ implanted; (b) Ce^+ implanted and then oxidized for 20 h; (c) 1 h pre-oxidized, Ce^+ implanted and then oxidized for 20 h

alloy interface is similar to that in the alloy. Cr is depleted at the interface. The distribution of Ce in the scales is different in Fig.6(b) and (c), which implies that corresponding two specimens have a different oxidation process. If the implanted Ce is taken as a built-in inert marker, the appearance of Ce peak in the outer layer of the oxide scale suggests that the location of new oxide formation is at the oxide/alloy interface. Therefore, for the direct implanted specimen, the inward diffusion of O^{2-} is predominant in the oxidation process. For the 1 h pre-oxidized and then implanted specimen, Ce distributes evenly in the outer region of the scale. So it can be proposed that during oxidation, the oxide growth on this sample involves the inward diffusion of oxygen in the RE-affected region and the outward diffusion of cations in the RE-unaffected region, where the former might be more prominent due to the overall higher concentration of Ce in the outer part of the scale.

3.4 Effects of implanted Ce

Based on the above results and the knowledge of the oxidation of Cr_2O_3 forming alloys, the oxidation process of GH128 alloy can be described as follows. At the initial stage, Cr_2O_3 grows on the surface, then NiO begins to form and reacts with Cr_2O_3 to form $NiCr_2O_4$ because of not enough Cr content in the alloy, i.e. the outward diffusion of Cr^{3+} and Ni^{2+} is predominant. In the oxidation process of the Ce directly implanted alloy, the inward diffusion of oxygen becomes the predominant step, correspondingly the oxidation rate is greatly reduced[3−5].

In the oxidation process of the pre-oxidized and then implanted GH128, both oxygen inward diffusion and cation outward diffusion happen. If the oxygen inward diffusion is a rate controlled step, the oxidation rate could be decreased, just as the case occurred on the 1 h pre-oxidized and then implanted GH128. Obviously, the beneficial effect of implanted Ce is related to the pre-oxidation time or preformed oxide thickness. According to the mechanism of “modification to oxide growth processes”[3−5], reactive elements play their beneficial effect through retarding cation boundary diffusion due to their segregation at oxide grain boundaries. With increasing the pre-oxidation time, the grain size of preformed oxides increases, and the content of dissolved Ce at the oxide grain boundaries reduces [11], so the retarding of implanted Ce in the RE-affected region for the cation outward diffusion becomes weak, even totally losses. Therefore, for the 5 h pre-oxidized and then implanted specimen, the inward diffusion of oxygen through the Ce incorporated oxide layer is not any more a subsequent oxidation control step, and its oxidation rate is similar to that of the blank GH128. The effect of REs on the oxidation rate of alloys is related with their existing states. The further work is needed to clarify the relationship of the grain boundary properties with the RE’s segregation.

Ce ion implantation exerts its beneficial effect on the spallation resistance of the oxide scales mainly through enhancing the strength of the oxide/alloy interface[8], such as retarding the formation of voids at

the oxide/alloy interface, developing a wavy configuration of the interface[13], and/or inhibiting sulfur segregation at the interface[6]. During the subsequent oxidation of the 1 h pre-oxidized and then implanted specimen, although the outward diffusion of Cr^{3+} and Ni^{2+} still happens, the voids formed due to the condensation of cation vacancies at the oxide/alloy interface should decrease under the condition of the low oxidation rate. Consequently, the oxide adhesion should be improved to some extent. According to this proposal, the slower the oxidation rate, the more obvious the oxide adhesion is improved. However, the different influence of Ce implantation into the blank and pre-oxidized specimens has not been found in the period of the cyclic oxidation. Much longer oxidation time may be needed.

It is shown clearly in Fig.4 that the configuration of the oxide/alloy interface of the three Ce implanted specimens is very wavy, and that of the blank GH128 is relatively smooth. The same phenomenon was found previously by HOU et al[14]. It was thought that this kind of the oxide/alloy interfaces improved the oxide adhesion by impeding crack propagation[15]. Therefore, the formation of the wavy interface is believed to be another important reason for improving the adherence of the scales on the Ce implanted GH128 with or without pre-oxidation.

It was verified that sulfur segregation at an oxide/metal interface weakens interfacial bonding[6]. In this study, it can be supposed that Ce does not get to the oxide/alloy interface for the pre-oxidized samples. The beneficial effect of Ce ion implantation on the growth rate and adhesion of the oxide scales on the pre-oxidized GH128 demonstrates that sulfur getting is not the main effect of Ce here. Rather, the change of the oxidation process owing to the segregation of Ce at the oxide grain boundaries is likely to be the main mechanism.

4 Conclusions

1) Ce^{+} implantation into the preformed oxide scale with the thickness of 0.6 μm decreased the subsequent oxidation rate of GH128 at 1 000 ℃ in air. When the thickness of the preformed scale was 1.3 μm, this beneficial effect no more existed.

2) In the case of the cyclic oxidation at 1 000 ℃ for 600 h, Ce implantation played a similar beneficial effect on the spallation resistance of the oxide scale on the blank and pre-oxidized GH128 alloy.

3) The improvement of oxide adhesion for pre-oxidized and then implanted GH128 was related to the formation of wavy oxide/alloy interfaces, not to the interfacial segregation of indigenous sulfur.

Acknowledgement

The authors greatly acknowledge Dr. P. Y. HOU for her useful suggestions and manuscript revision.

References

[1] WHITTLE D P, STRINGER J. Improvements in high temperature oxidation resistance by additions of reactive elements or oxide dispersions [J]. Philos Trans R Soc London, 1980, A295(1413): 309−329.

[2] PINT B A. Experimental observation in support of the dynamic-segregation theory to explain the reactive-element effect [J]. Oxid Met, 1996, 45: 1−37.

[3] COTELL C M, YUERK G J, HUSSEY R J, MITCHHELL D F, GRAHAM M J. The influence of implanted yttrium on the mechanism of growth of Cr_2O_3 on Cr [J]. J Electrochem Soc, 1987, 134(7): 1871−1872.

[4] PRZYBYLSKI K, GARRAT-REED A J, YUREK G J. Grain boundary segregation of yttrium in chromia scales [J]. J Electrochem Soc, 1988, 135(2): 509−517.

[5] NAGAI H, OKABAYASHI M. High-temperature oxidation of Ni-20Cr alloys with dispersion of various reactive metal oxides [J]. Trans Jpn Inst Met, 1981, 22(2): 101−108.

[6] HOU P Y. Beyond the sulfur effect [J]. Oxid Met, 1999, 52: 337−351.

[7] LEES D G. On the reasons for the effects of dispersions of stable oxides and additions of reactive elements on the adhesion and growth-mechanisms of chromia and alumina scales—The "sulfur effect" [J]. Oxid Met, 1987, 27(1/2): 75−81.

[8] HOU P Y, BROWN I G, STRINGER J. Study of the effect of reactive-element addition by implanting metal ions in a preformed oxide layer [J]. J Nucl Instrum Meth, 1991, B59/60: 1345−1349.

[9] PAÚL A, ELMRABET S, AGER F J, ODRIOZOLA J A, RESPALDIZA M A, DA SILVA M F, SOARES J C. Influence of preoxidation and annealing treatments on the isothermal oxidation in air at 1 173 K of cerium-implanted EN-1.4301 stainless steel [J]. Oxid Met, 2002, 57: 33−51.

[10] LI Mei-shuan, QIAN Yu-hai, LI Ya-li, ZHOU Yan-chun. Beneficial effects of Ce implantation into preformed Cr_2O_3 scales on the subsequent oxidation of Ni-20Cr alloy [J]. Oxid Met, 2004, 61: 529−544.

[11] LI M S, HOU P Y. Improved Cr_2O_3 adhesion by Ce ion implantation in the presence of interfacial sulfur segregation [J]. Acta Mater, 2007, 55: 443−453.

[12] MCHARGUE C J. Ion implantation in metals and ceramics [J]. Inter Metals Reviews, 1986, 31(2): 49−76.

[13] RAHMEL A, SCHÜTZE M. Mechanical aspects of the rare-earth effect [J]. Oxid Met, 1992, 38(3/4): 255−266.

[14] HOU P Y, CHIA V, BROWN I. Distribution of ion-implanted yttrium in Cr_2O_3 scales and in the underlying Ni-25wt.%Cr alloy [J]. Surf Coat Technol, 1992, 51: 73−78.

[15] WOOD G C, RICHARDSON J A, HOBBY M G, BOUSTEAD J. The identification of thin healing layers at the base of oxide scales on Fe-Cr base alloys [J]. Corr Sci, 1969, 9: 659−671.

(Edited by YUAN Sai-qian)